frontiers | Frontiers in Molecular Biosciences

TYPE Original Research
PUBLISHED 17 August 2023
DOI 10.3389/fmolb.2023.1214102

OPEN ACCESS

EDITED BY
Nicole Perry-Hauser,
Columbia University, United States

REVIEWED BY
Zhenhua Shao,
Sichuan University, China
Eugenia Gurevich,
Vanderbilt University, United States
Jeffrey Smith,
Harvard Medical School, United States

*CORRESPONDENCE
Rachel A. Matt,
matt@curasen.com

†These authors have contributed equally to this work

RECEIVED 28 April 2023
ACCEPTED 05 July 2023
PUBLISHED 17 August 2023

CITATION
Matt RA, Westhorpe FG, Romuar RF, Rana P, Gever JR and Ford AP (2023), Fingerprinting heterocellular β-adrenoceptor functional expression in the brain using agonist activity profiles. *Front. Mol. Biosci.* 10:1214102. doi: 10.3389/fmolb.2023.1214102

Fingerprinting heterocellular β-adrenoceptor functional expression in the brain using agonist activity profiles

Rachel A. Matt*†, Frederick G. Westhorpe†, Rosemary F. Romuar, Payal Rana, Joel R. Gever and Anthony P. Ford

Department of Pharmacology, CuraSen Therapeutics, San Carlos, CA, United States

Noradrenergic projections from the brainstem locus coeruleus drive arousal, attentiveness, mood, and memory, but specific adrenoceptor (AR) function across the varied brain cell types has not been extensively characterized, especially with agonists. This study reports a pharmacological analysis of brain AR function, offering insights for innovative therapeutic interventions that might serve to compensate for locus coeruleus decline, known to develop in the earliest phases of neurodegenerative diseases. First, β-AR agonist activities were measured in recombinant cell systems and compared with those of isoprenaline to generate $\Delta\log(E_{max}/EC_{50})$ values, system-independent metrics of agonist activity, that, in turn, provide receptor subtype fingerprints. These fingerprints were then used to assess receptor subtype expression across human brain cell systems and compared with $\Delta\log(E_{max}/EC_{50})$ values arising from β-arrestin activation or measurements of cAMP response desensitization to assess the possibility of ligand bias among β-AR agonists. Agonist activity profiles were confirmed to be system-independent and, in particular, revealed β_2-AR functional expression across several human brain cell types. Broad β_2-AR function observed is consistent with noradrenergic tone arising from the locus coeruleus exerting heterocellular neuroexcitatory and homeostatic influence. Notably, $\Delta\log(E_{max}/EC_{50})$ measurements suggest that tested β-AR agonists do not show ligand bias as it pertains to homologous receptor desensitization in the system examined. $\Delta\log(E_{max}/EC_{50})$ agonist fingerprinting is a powerful means of assessing receptor subtype expression regardless of receptor expression levels or assay readout, and the method may be applicable to future use for novel ligands and tissues expressing any receptor with available reference agonists.

KEYWORDS

adrenergic, noradrenergic, GPCR, biased agonism, agonist, desensitization, receptor, expression

1 Introduction

The β-adrenergic receptor (β-AR) family comprises three established targets of successful therapeutics for patients with respiratory, cardiovascular, and urological disorders (Wachter and Gilbert, 2012; Camoretti-Mercado and Lockey, 2019). Historically, β-ARs have not been targeted for central nervous system-acting therapeutics, despite implications of early decline of noradrenergic tone in neurodegenerative disease (Leanza et al., 2018; Magistrelli and Comi, 2019). Brain β-ARs

are activated by noradrenaline released principally from diffuse neuronal projections arising from the pontine locus coeruleus (LC) (Brunnström et al., 2011; Schwarz and Luo, 2015). The LC is especially vulnerable to neurodegenerative processes. It is the first brain region tau pathology of Alzheimer's disease emerges (Braak et al., 2011) and one of the first to show alpha-synuclein/Lewy body pathology; subsequent loss of noradrenergic neurons is progressive and correlated with decline in cognitive function (Mather and Harley, 2016; Matchett et al., 2021). Noradrenergic tone is essential for wakefulness, arousal, regulation of sleep and mood, memory, and impulsive behaviors (Berridge and Waterhouse, 2003; Aston-Jones and Cohen, 2005; Bari and Robbins, 2013; Mather et al., 2016; Roozendaal and Hermans, 2017; Hayat et al., 2020). As excitatory targets of noradrenergic neurotransmission, β-ARs are known to have important neuronal (Mather et al., 2016) and non-neuronal functions, including astrocytic maintenance of nutrition and metabolism (Hertz et al., 2010; Dienel and Cruz, 2016), modulation of the neurovascular unit (NVU) and maintenance of cerebral perfusion (Toussay et al., 2013; Froese et al., 2020), and regulation of inflammatory balance and microglial clearance of protein debris (Heneka et al., 2010; Feinstein et al., 2016; Ardestani et al., 2017; Evans et al., 2020). Recently, there has been increasing interest in the potential for restoring lost adrenergic tone in treatment of neurodegenerative diseases, including Parkinson's disease (O'Callaghan et al., 2021), with pharmacoepidemiology studies also supporting the β-AR family as promising therapeutic targets in humans (Mittal et al., 2017; Gronich et al., 2018; Cepeda et al., 2019; Koren et al., 2019).

Detailed characterization of the functional expression of distinct β-AR populations in glial and non-glial cells is important to predict their suitability as potential therapeutic targets. Changes in receptor expression level or coupling efficiency between systems, and the resulting changes in agonist potency and maximal efficacy values, can confound translatability of agonist impact for drug development programs. Should novel, brain directed, β-AR agonist therapeutics be developable, translational methods will be crucial for comparing agonist profiles, understanding differential receptor expression across different tissues, and modeling the impact on brain function from preclinical data to clinical data.

One recent analytical advancement for the pharmacologist is the use of $\log(E_{max}/EC_{50})$ (Kenakin, 2017), which has demonstrated utility in examining ligand bias across several receptor families (including G protein-coupled receptor (GPCR) and non-GPCRs) (Karl et al., 2020; Griffith et al., 2022; Reininghaus et al., 2022), as well as meta-analysis of GPCR: G protein coupling (Hauser et al., 2022). In these methods, agonist action is compared to that of a reference agonist, from which $\Delta\log(E_{max}/EC_{50})$ values are derived, allowing cell- or assay-specific features to be neutralized and permitting agonist activity translation across systems. Using cAMP concentration–response curves, we calculated isoprenaline-referenced $\Delta\log(E_{max}/EC_{50})$ values for established β-AR agonists for each of the three different β-AR subtypes (β_1-AR, β_2-AR, and β_3-AR), expressed recombinantly. These data generated an "agonist fingerprint" for each β-AR subtype functionally expressed. We then used this fingerprint to assess functional expression in previously uncharacterized central nervous system (CNS) relevant cell lines, iPSC-derived human brain cell types and primary human glia. We also used $\Delta\log(E_{max}/EC_{50})$ to assess β-arrestin recruitment and desensitization, key components of the cycle of GPCR activation and inactivation (Luttrell and Lefkowitz, 2002).

Together, this work provides an in-depth characterization of signaling responses to β-AR agonists and further tests the use of $\Delta\log(E_{max}/EC_{50})$ analysis as a framework for characterizing GPCR expression and function. We demonstrate that β_2-AR functional expression is most widespread among isolated cell types from the human brain, and our data suggest that established β-AR agonists are essentially unbiased in their activation of β_2-AR for Gs versus β-arrestin and signal desensitization. This characterization provides an important reference for further *in vitro* functional studies of adrenoceptor activation in the human brain.

2 Materials and methods

2.1 Compound sources and handling

Compounds were sourced as follows: isoprenaline (TCI I0260), adrenaline (Sigma E4250), noradrenaline (Matrix Scientific 037592), dobutamine (Tocris 0515), prenalterol (Santa Cruz Bio sc-280023), formoterol (Apex Bio B1359), clenbuterol (Sigma C5423), salbutamol (Sigma S8260), tulobuterol (Alfa Aesar J61448), and mirabegron (Med Chem Express CS-0915). Upon arrival, ~2 mg of the compound was weighed out and resuspended in DMSO to achieve a final concentration of 10 mM. Compounds were aliquoted and stored at −80°C or −20°C until use. A limit of five freeze/thaw cycles was implemented for each aliquot.

2.2 Cell culture

All cell sources, exogenous protein expression information, and growth media conditions are detailed in Supplementary Table S1. All cells were grown in a 37°C, 5% CO_2 humidified incubator. Any CHO-K1 cell line recombinantly expressing a receptor transgene was grown in media supplemented with 1 mg/mL G418 (Sigma A1720) to maintain selection for transgene expression.

2.3 Cell engineering

CHO-K1 cell transgene lines engineered at CuraSen were all prepared from human codon-optimized, gene-synthesized constructs (GenScript) corresponding to sequences with protein accession numbers detailed in Supplementary Table S1. Genes were NotI/XbaI restriction digested into the pCMV6KN expression vector (OriGene) and transfected into CHO-K1 cells using Lipofectamine 3000, following the manufacturer's instructions. Up to 1 mg/mL G418 (Sigma A1720) was supplemented to media 48 h post transfection to positively select for and maintain transfected cells.

Monoclonal cell lines were generated by dilution cloning. In brief, single cells were grown in 96-well plates, allowed to proliferate into stable cultures, and assessed for receptor expression by again assessing the responses to established receptor agonists.

To create THP-1 cells expressing only β_1-AR or β_2-AR, the β_2-AR or β_1-AR coding gene (ADRB1 or ADRB2, respectively) was

knocked out using CRISPR/Cas9 (Synthego). THP-1 cells were nucleofected with optimized sgRNA/SpCas9 ribonucleoprotein complexes, with the ADRB1 or ADRB2 gRNA target sequences: GCGGCCCCACACCACGAUGG and CGUCUGCAGACGCUC GAACU, respectively. The indel percentage in the cell population after knockout was 65% and 67%, from which monoclonal cell populations were grown in-house as previously described to identify and isolate knockout clones.

To create C6 rat glioma cells expressing only β_1-AR, the β_2-AR coding gene (*Adrb2*) was knocked out using CRISPR/Cas9 (Synthego). C6 cells were nucleofected with optimized sgRNA/SpCas9 ribonucleoprotein complexes with the *Adrb1* or *Adrb2* gRNA target sequence: GCUGCUGCCUCCAGCCAGCG and CCUGGCGCUCGGCUUCCAUU. The indel percentage in the cell population after knockout was 65% and 85%, from which monoclonal cell populations were grown in-house as previously described to identify and isolate knockout clones.

ReNcell VM cells expressing β_2-AR were generated by infecting ReNcell VM cells with a lentivirus containing the ADRB2 gene (OriGene RC204499L3V) at an MOI of 12.5, and 48 h post-infection, cells were grown in media containing 0.25 μg/mL puromycin.

To passage adherent cells, cells were released either using EDTA solution (Versene, Lonza 17-711E) after washing in 1x PBS (Caisson PBL05) or using Accutase (Mediatech 25-058-CI) after washing in 1x PBS.

2.4 cAMP HTRF assay

cAMP accumulation was measured using the cAMP Gs Dynamic HTRF kit (Cisbio/Perkin Elmer 62AM4PEC), broadly following the manufacturer's instructions. Compounds were prepared at a 2x final concentration to accommodate the subsequent addition of cells. To prepare compound dose–response curves, compounds were diluted to the necessary highest concentration (default 10 μM, but dependent on compound potency) in 1x stimulation buffer containing 500 μM 3-isobutyl-1-methylxanthine (IBMX) and dispensed into a 96-well U-bottom polypropylene assay plate (Corning 3365). Vehicle (DMSO), a maximally active isoprenaline dose (0.1 μM for β_1-AR and β_2-AR and 1 μM for β_3-AR), and a full isoprenaline dose–response curve were added as controls on all assay plates. β-AR agonists were serially diluted across the plate by nine 5-fold dilutions to generate a 10-point dose–-response curve.

Five microliters from 96-well compound source plates were stamped into every well of a 384-well white-bottom plate (Corning 3825) using a VIAFLO 384 equipped with a 0.5–12.5 μL pipetting head (Integra), thus creating four technical replicates for each treatment condition. Plates (384-well) containing compounds were covered and stored at room temperature until addition of resuspended cells.

D2-labeled cAMP (acceptor) and europium cryptate-labeled cAMP antibody (donor) (Cisbio/Perkin Elmer 62AM4PEC) were dissolved in water following the manufacturer's instructions, aliquoted, and stored at −80 °C. For detection of cAMP, on the day of the assay prior to addition of cells to compounds, both reagents were diluted 21-fold in the provided lysis buffer (Cisbio/Perkin Elmer), combined, and stored at room temperature prior to addition to assay plates.

Resuspended cells were resuspended in a minimal volume of 1x stimulation buffer containing 500 μM IBMX at room temperature. All cell suspensions were further diluted in 1x stimulation buffer containing 500 μM IBMX to a density corresponding to the lower values of the dynamic range of the cAMP HTRF assay, with each cell system optimized individually. Five microliters of cells of correct density were added to the compound in assay plates using a Multidrop Combi (Thermo Fisher). Cells and compounds were covered with a clear plate seal (Axygen PCR-SP) and incubated at 37°C, 5% CO_2 for 30 min. cAMP accumulation was then stopped by adding 10 μL HTRF detection reagents in lysis buffer using the Multidrop Combi and plates were covered with an aluminum plate seal (Axygen PCR-AS-600) and agitated (Heidolph Titramax 1000, setting 600) for at least 2 h, to allow competition between D2-cAMP and stimulated cAMP for the donor-labeled cAMP antibody to reach equilibrium.

HTRF was detected using a Tecan Spark plate reader, operated using SparkControl™ software, using the TR fluorescence intensity setting. Both the donor and acceptor were excited at 320 nm, detected after 100-μs delay, with 400-μs integration time, and 50 flashes per read. Donor fluorescence was detected at 620 nm, and acceptor fluorescence was detected at 665 nm. To standardize reads across experiments, camera gain was manually set to 120 for donor detection and 140 for acceptor detection.

2.5 cADDis assay

cADDis fluorescence assays were performed broadly as described by the manufacturer (Montana Molecular D0200G). A single cADDis infection reaction comprised 25 μL cADDis mix (3.75 μL cADDis sensor BacMam, 0.3 μL 500 mM sodium butyrate, and 20.95 μL 'cADDis media' (FluoroBrite media + GlutaMAX (Gibco) + 10% FBS, 1% P/S)), combined with 25 μL cADDis media containing 1321N1 cells at a density of 6×10^4 cells/mL. A mixture of cADDis reaction and 1321N1 cells was prepared to provide enough volume to seed the middle 240 wells of a 384-well plate (Corning 3764). Using a VIAFILL (Integra) equipped with a 16-channel head, 50 μL of cADDis: 1321N1 cells was added to each well (1,500 cells per well), and the plate was incubated at room temperature for 15 min before overnight incubation in a 37°C, 5% CO_2 humidified incubator.

After 24 h of incubation, cells were imaged using an Incucyte S3 (green and phase channel) to measure cADDis fluorescence intensity at baseline (unstimulated). Compounds were diluted to the 5x final concentration in cADDis media, serially diluted while maintaining vehicle (DMSO) concentration, and 12.5 uL of 5x compound was seeded into the cADDis 1321N1 cell plate using a VIAFLO 384 (Integra). The 1321N1 cells were immediately imaged again on the Incucyte (the final image time point was 10 min post drug addition).

For each well, the cADDis intensity after compound addition was normalized to the mean of the vehicle control wells, and this intensity was corrected for the cADDis intensity of that well at baseline (pre-compound addition, Time 0) as it related to the mean baseline intensity of all wells across the test plate.

2.6 Isoprenaline $\Delta\log(E_{max}/EC_{50})$ analysis and radar plot generation

β-AR agonist $\log(E_{max}/EC_{50})$ values were calculated for each concentration–response curve using GraphPad Prism and Microsoft Excel. A reference agonist (isoprenaline) dose–response curve was generated in the same plate as each test agonist, on the same experimental day with identical cell and assay reagents. Therefore, β-AR agonist $\Delta\log(E_{max}/EC_{50})$ values, relative to isoprenaline, were also calculated on a plate-matched basis. Average isoprenaline $\Delta\log(E_{max}/EC_{50})$ values for each β-AR agonist were used to generate β-AR fingerprint radar plots of system responses to β-AR agonists, again using Microsoft Excel. Therefore, radar plots reflect $\Delta\log(E_{max}/EC_{50})$ mean values calculated from the entire dataset presented in Supplementary Table S2, which contains both tandem- (different test agonists evaluated on different experimental days) and parallel-design (panel of agonists assayed on the same experimental day) experiments, but where each $\Delta\log(E_{max}/EC_{50})$ value is calculated on a plate-matched basis.

A comparison between $\Delta\log(E_{max}/EC_{50})$ error calculations using tandem versus parallel experimental design is shown in Supplementary Table S3. The first method is identical to that shown for the full dataset in Supplementary Table S2, reflecting the nature of plate-matched $\Delta\log(E_{max}/EC_{50})$ values, and the second method follows that described in Kenakin et al. (2012). The latter method is included to inform any uses of this reference dataset in an experimental design, which would not allow technical matching of test and reference agonists.

2.7 DiscoverX PathHunter® arrestin recruitment assay

DiscoverX PathHunter® cells expressing β_2-AR (93–0182C2) with a receptor ProLink™ tag and arrestin enzyme acceptor tag were cultured in T75 flasks at 37°C, 5% CO_2 in a growth medium containing DMEM/F12 (Caisson Labs DFL13), 10% FBS (Corning 35-010-CV), 1x penicillin/streptomycin (Caisson Labs PSL01), 1 mg/mL G-418 (Caisson Labs G030), and 300 μg/mL hygromycin (Caisson Labs H010) and were passaged before full confluence. Cells were seeded in 384-well plates (Corning 3570) at a density of 5,000 cells per well in 20 μL growth medium. The next day, solutions of β-AR agonist were prepared as 5-fold serial dilutions in a 96-well plate (Corning 3363) at the desired final concentration of 5x. About 5 μL of the drug solution was transferred from this 96-well source plate to the 384-well cell plate using a VIAFLO 384 equipped with a 0.5–12.5 μL pipetting head (Integra), generating four technical replicates for each drug dose. Plates were sealed with clear plastic (Corning AXYPRSP) and incubated for 90 min in a 37°C, 5% CO_2 incubator. Meanwhile, the working detection solution (WDS) was freshly prepared at room temperature from kit reagents (93-0001L) as per the manufacturer's instructions in a 19:5:1 ratio (buffer: component 1: component 2). After drug incubation was complete, 12.5 μL WDS was added per well using a Multidrop Combi. Plates were covered with an aluminum plate seal (Axygen PCR-AS-600) and agitated (Heidolph Titramax 1000, setting 600) for 90 min. Luminescence was detected (360–700 nm) with a Tecan Spark plate reader, operated using SparkControlTM software, using 500 ms integration time.

2.8 Functional desensitization assay

1321N1 cells were seeded in 384-well plates (Corning 3570 or 3764) at a density of 5,000 cells per well in 40 μL growth medium. The next day, solutions of β-AR agonists were prepared as 5-fold serial dilutions in a 96-well plate to the desired final concentration of 5x. About 10 μL of the drug solution was transferred from the 96-well source plate to the 384-well cell plate using a VIAFLO 384 equipped with a 0.5–12.5 μL pipetting head (Integra), generating four technical replicates for each drug dose. A full concentration–response curve of isoprenaline was prepared for each cell plate to allow in-plate determination of $\Delta\log(E_{max}/EC_{50})$. Cells were incubated with 1x drug solution for 24 h. After 24 h of incubation, cells were washed three times by inverting and gently tapping plates onto paper towels, followed by centrifugation of the inverted plate at 30 x g, before adding 40 μL of wash solution containing DPBS, + 0.1% bovine serum albumin (VWR 97061-416) using a VIAFILL dispenser (Integra). After the third wash solution removal, 10 μL of a solution of HTRF Stimulation Buffer 1 (Cisbio/Perkin Elmer 64SB1FDC) containing 500 μM IBMX (Cayman 13347) and 5 μM tulobuterol was added to each well with a VIAFLO pipette. The cell plate was sealed with clear plastic and incubated at 37°C for 30 min. D2-labeled cAMP (acceptor) and europium cryptate-labeled cAMP antibody (donor) (Cisbio/Perkin Elmer 62AM4PEC) were dissolved in water and added to cell plates as previously described for the cAMP HTRF assay, followed by similar signal detection using a Tecan Spark plate reader.

2.9 Data and statistical analysis

Concentration–response curves shown in figures display mean ± SEM across n = 4 technical replicates from a single representative dose–response curve. For dose–response curves generated from cAMP HTRF, raw ratiometric HTRF signals, relative to the maximum effect of isoprenaline, were plotted, unless stated. Each compound was assayed a minimum of three times in independent experiments. The exact experimental replicate number is shown in Supplementary Table S2. Correlation plots (Figures 6 and 7) show mean $\Delta\log(E_{max}/EC_{50})$ values ± 95% CI across n = 3 independent experiments.

cAMP HTRF ratios were obtained by applying the formula

$$(\text{Abs}(665\text{ nm})/\text{Abs}(620\text{ nm}))\text{ x }10,000,$$

where Abs (665 nm) and Abs (620 nm) are the absolute fluorescence units detected at 665 nm (HTRF acceptor) and 620 nm (HTRF donor), respectively.

For all dose–response curves generated across all assay readouts (cAMP HTRF and cADDis), the potencies of test and control compounds were determined by non-linear regression using GraphPad Prism. HTRF ratios, from quadruplicate measures at each concentration, were plotted versus the log concentration of β-AR agonist and analyzed using the following 4-parameter logistic equation:

$$y = Bottom + \frac{x^{Hill\ slope} \cdot (Top - Bottom)}{x^{Hill\ slope} + EC_{50}{}^{Hill\ slope}}. \quad (1)$$

All dose–response curves on a given plate were simultaneously analyzed to define a single, shared baseline value, and the Hill slope was constrained to be >0, to avoid false curve fits from inactive compounds. The average (mean) β-AR agonist potency (pEC_{50}) and maximum effect (E_{max}) relative to the within-plate isoprenaline dose response were reported.

For normalizing cAMP HTRF ratiometric data to a cAMP standard curve, cAMP (Sigma A6885) was dissolved, and a concentration range was prepared by serial dilution in 1x stimulation buffer. The cAMP standard curve was detected by cAMP HTRF contemporaneously with β-AR agonist-stimulated 1321N1 cells, as described previously. The cAMP standard curve was fitted to a non-linear regression 4-parameter logistic equation as described previously, with a separate baseline value from β-AR agonist dose responses in cells. The standard curve was used to interpolate per-well cAMP quantities from raw ratiometric cAMP HTRF values for each dose of each β-AR agonist. β-AR agonist cAMP-normalized concentration dose–response curves were then analyzed using 4-parameter logistic regression, as described previously, to assess the potency and efficacy of compounds.

Representative dose–response curves shown were compiled from raw cAMP HTRF ratiometric values, first by selecting individual agonist dose responses that closely resembled average potency and maximal efficacy values. Those selected datasets were normalized to the plate-matched isoprenaline dose–response curve, first by calculating the individual cAMP HTRF ratio value relative to the average of the isoprenaline baseline (lowest concentration isoprenaline value) and then by dividing that value by the average maximal (highest concentration isoprenaline value) isoprenaline response to make the isoprenaline dose–response curve 100%.

To assess β-AR agonist selectivity at β_1-AR versus β_2-AR, average β-AR agonist $\Delta\log(E_{max}/EC_{50})$ values, relative to isoprenaline, for β_2-AR (in CHO-K1 cells) were subtracted from the average β-AR agonist $\Delta\log(E_{max}/EC_{50})$ values, relative to isoprenaline, for β_1-AR (again in CHO-K1 cells) to generate $\Delta\Delta\log(E_{max}/EC_{50})$ values (Supplementary Table S4). This analysis was performed on a subset of six experiments run in parallel, where all agonists and cell lines displayed were tested on the same experimental day. $\Delta\Delta\log(E_{max}/EC_{50})$ values were also calculated for cAMP, arrestin recruitment, and functional desensitization assays (Supplementary Table S4). 95% confidence intervals were calculated according to the method described in Kenakin et al. (2012) and Servant et al. (2022).

3 Results

3.1 Recombinant cell systems define agonist fingerprints for β-AR subtype functional expression

We first established a reference agonist activity dataset in recombinant β-AR expression systems. The activity of β-AR agonists was measured by detecting cAMP increases in CHO-K1 cells expressing either β_1-, β_2-, or β_3-AR human homologs. We characterized the endogenous β-AR agonists adrenaline and noradrenaline, the potent and non-selective β_1/β_2-AR agonist isoprenaline, β_1-AR selective agonists dobutamine and prenalterol, β_2-AR selective agonists salbutamol, clenbuterol, tulobuterol, and formoterol, and the β_3-AR selective agonist mirabegron. As a negative control, CHO-K1 cells lacking recombinant expression showed no cAMP response to any agonist tested (Supplementary Figure S1).

For each concentration–response curve, ratiometric cAMP HTRF values were normalized to the maximal response of isoprenaline, which was selected as the reference full agonist throughout our study. Representative dose–response curves of β-AR activation in CHO-K1 cells and summary data are shown in Figures 1A–C, and summary data are shown in Figure 1D. β-AR activation was observed at all three β-AR subtypes in response to all β-AR agonists tested.

For each agonist in each replicate experiment, we calculated the $\log_{10}$-transformed E_{max}/EC_{50} ratio (Equation 2: Emax as a fraction of the reference agonist; EC_{50} expressed in M units). We then subtracted the same metric of the plate-matched reference agonist, isoprenaline, for which E_{max} is defined as 1.

$$\Delta\log\left(\frac{E_{max}}{EC_{50}}\right) = \log\left(\frac{E_{max}}{EC_{50}}\right)_{test\ agonist} - \log\left(\frac{E_{max}}{EC_{50}}\right)_{isoprenaline} \quad (2)$$

The resulting value, hereby referred to as $\Delta\log(E_{max}/EC_{50})$, provides a system-independent metric for agonist activity relative to isoprenaline (Kenakin, 2017), provided Hill slopes are near unity (Winpenny et al., 2016).

$\Delta\log(E_{max}/EC_{50})$ is, in theory, independent of tissue, assay, and receptor coupling, as variations in receptor expression, amplification, or other variables are canceled by the comparison to a reference agonist (Kenakin, 2017). Accordingly, $\Delta\log(E_{max}/EC_{50})$ values across a panel of agonists provide a composite readout of receptor activation by those agonists as a profile. $\Delta\log(E_{max}/EC_{50})$ values were arranged in a radar plot to give each β-AR population a distinct visual agonist fingerprint (Figures 1E–G for the three recombinant human β-ARs), which could then be compared across other cell system assays. In this agonist fingerprint, values further from the center represent greater activity, while values closer to the center represent lower activity, all relative to isoprenaline, for which the $\Delta\log(E_{max}/EC_{50})$ is 0. The exact shape of the agonist fingerprint is arbitrary, as it depends on the agonist arrangement on the radar axes. Imposing a fixed orientation of agonists on the plot, the shape of the fingerprint is unique for each receptor subtype. The resulting $\Delta\log(E_{max}/EC_{50})$ β-AR agonist fingerprints allow functional expression of the three β-ARs to be easily distinguished from one another.

$\Delta\log(E_{max}/EC_{50})$ analysis may also be used to analyze selectivity for any of the test agonists for one receptor subtype over another, by comparing $\Delta\log(E_{max}/EC_{50})$ values across two assay systems ($\Delta\Delta\log(E_{max}/EC_{50})$) (Kenakin, 2017). Interpretation of selectivity using $\Delta\Delta\log(E_{max}/EC_{50})$ is relative to the reference agonist, so it is optimal when that reference agonist is thought to be non-selective between receptors being examined. As isoprenaline is thought to be non-selective at β_1-AR vs. β_2-AR (Baker, 2010), we examined β_1-AR vs. β_2-AR selectivity using $\Delta\Delta\log(E_{max}/EC_{50})$ (Supplementary

10.3389/fmolb.2023.1214102

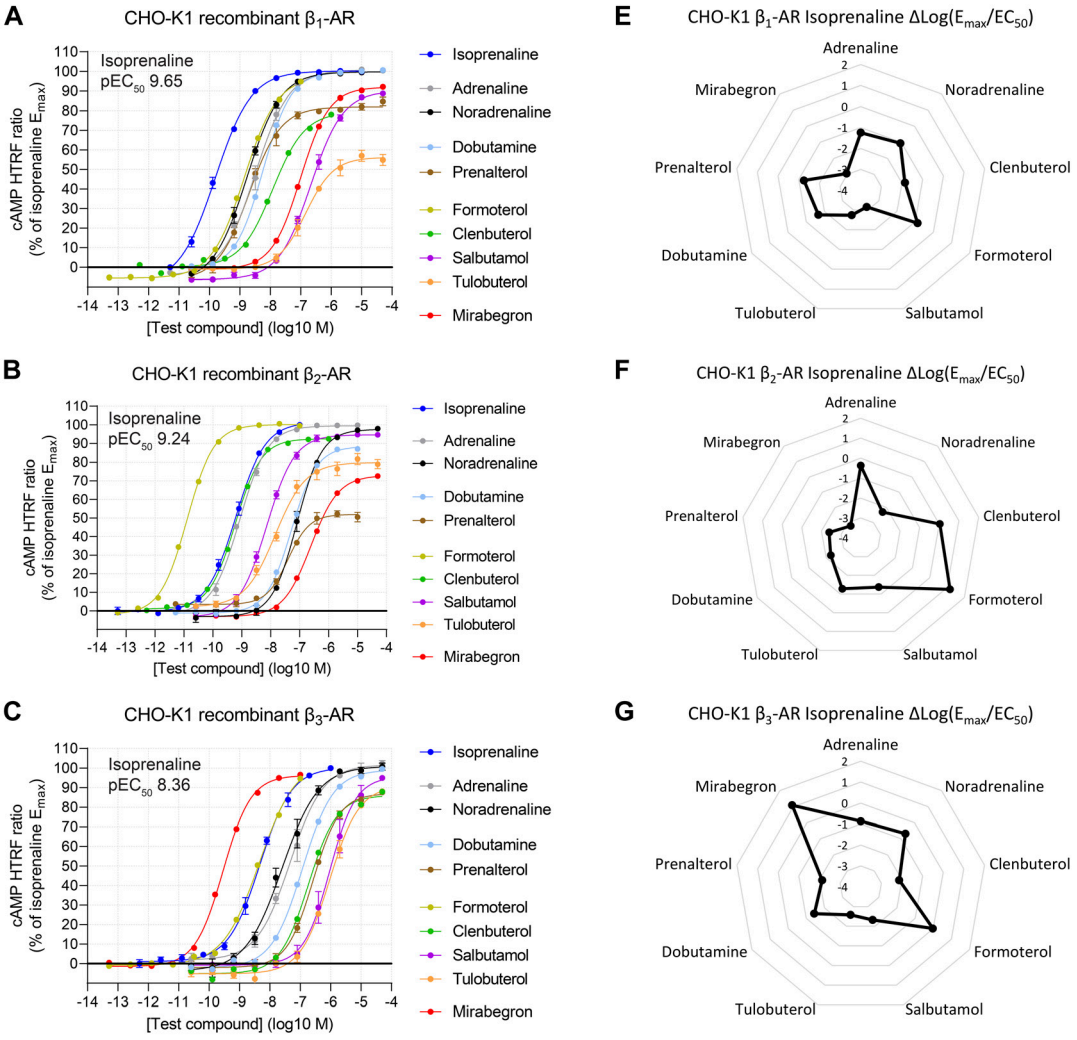

D

β-AR agonist	CHO-K1 recombinant β_1-AR			CHO-K1 recombinant β_2-AR		
	pEC_{50}	Emax (% isoprenaline)	Isoprenaline $\Delta\log(E_{max}/EC_{50})$	pEC_{50}	Emax (% isoprenaline)	Isoprenaline $\Delta\log(E_{max}/EC_{50})$
Isoprenaline	9.65	100	0	9.24	100	0
Adrenaline	8.44	101	-1.24	8.89	101	-0.36
Noradrenaline	8.6	101	-1.06	6.96	100	-2.3
Dobutamine	8.02	99	-1.67	7.16	80	-2.26
Prenalterol	8.56	82	-1.25	7.4	30	-2.39
Formoterol	8.91	99	-0.87	10.51	100	1.17
Clenbuterol	7.89	76	-1.86	9.28	91	0.03
Salbutamol	6.61	89	-3.16	7.98	96	-1.37
Tulobuterol	6.9	74	-2.74	7.91	76	-1.28
Mirabegron	7.02	91	-2.95	6.56	68	-3.21

FIGURE 1
Functional cAMP responses to a panel of β-AR agonists in CHO-K1 cell lines recombinantly expressing **(A)** β_1-AR, **(B)** β_2-AR, or **(C)** β_3-AR human receptors. Representative curves are displayed, each with four technical replicates, showing mean ± SEM cAMP HTRF responses normalized to the full agonist isoprenaline. Each agonist curve was converted to a $\Delta\log(E_{max}/EC_{50})$ agonist fingerprint using isoprenaline as the reference molecule **(D–G)**. This allows a system-independent visualization of agonist similarity to isoprenaline (nodes) and receptor expression (edges) across a range of isoprenaline potencies. A similar analysis in the endogenous expression system 1321N1 astrocytoma cell line reveals an agonist fingerprint, consistent with β_2-AR and not β_1-AR expression **(H)**. Average concentration–response curves for β_1-AR and β_2-AR across a subset of six experiments with agonists tested in parallel are shown in Supplementary Figure S2.

Figure S2) and found selectivity consistent with that of previous reports of Baker (2010). We did not assess selectivity involving β_3-AR, for which isoprenaline has lower potency (Baker, 2010). For this reason, and because we did not observe a β_3-AR fingerprint in all other cell lines described as follows, β_3-AR (and the agonist mirabegron) are not further discussed here.

3.2 Using agonist fingerprinting to define β-AR expression in native cell systems expressing single or multiple β-AR populations

The utility of $\Delta\log(E_{max}/EC_{50})$ agonist fingerprinting was assessed in a native expression system, 1321N1 astrocytoma cells: a human cell line reported to express β_2-AR (Su et al., 1979; Doss et al., 1981). β-AR agonist-driven cAMP responses were readily detectable in 1321N1 cells (Supplementary Figure S4D). β-AR agonist potency and E_{max} values in 1321N1 cells were different from the potency and E_{max} values measured in all CHO-K1 recombinant systems (Supplementary Table S2), consistent with decreased receptor reserve for the native cell-line versus recombinant cells.

We represented β-AR agonist activity in 1321N1 cells as a $\Delta\log(E_{max}/EC_{50})$ β-AR agonist fingerprint (Figure 1H). Agonists showing no response or incomplete curves were removed as axes in the radar plot. The 1321N1 β-AR agonist fingerprint matched that observed in the CHO-K1 recombinant system expressing β_2-AR, suggesting that 1321N1 cells indeed naturally express β_2-AR. We confirmed this result using selective β-AR antagonists, observing that the β_2-AR selective antagonist ICI-118,551 displayed a 10^5-fold lower inhibition constant (IC_{50}) versus the β_1-AR selective antagonist CGP-20712A (Supplementary Figure S3). These data confirm that 1321N1 cells natively express β_2-AR and validate, with real-world data, the use of $\Delta\log(E_{max}/EC_{50})$ as a method of assessing β-AR subtype functional expression independent of receptor expression density or coupling efficiency.

To test the performance of $\Delta\log(E_{max}/EC_{50})$ agonist fingerprinting using alternative cAMP detection assays, we employed cADDis (Montana Molecular), a live-cell fluorescent biosensor that decreases in fluorescence intensity when bound to cAMP (Tewson et al., 2016). We measured β-AR agonist activity in 1321N1 cells expressing cADDis and observed an agonist-mediated, dose-dependent decrease in cADDis fluorescence (Supplementary Figures S4A, B). The cADDis assay was less sensitive than cAMP HTRF detection methods, which limited the panel of β-AR agonists for which we could generate full dose–response curves. Nevertheless, measurable $\Delta\log(E_{max}/EC_{50})$ β-AR agonist values from cADDis matched $\Delta\log(E_{max}/EC_{50})$ values derived from cAMP HTRF, and therefore generated an identical β-AR agonist fingerprint to that derived from cAMP HTRF (Supplementary Figure S4C). These data confirm that $\Delta\log(E_{max}/EC_{50})$ activity determination is agnostic of the reagent used to measure agonist activation of cyclic AMP production.

Lastly, to ensure that normalization methods (Burford et al., 2017) do not affect the interpretation of $\Delta\log(E_{max}/EC_{50})$, we confirmed that dose–response curves derived from HTRF values pre- and post-normalization by a cAMP standard curve gave identical $\Delta\log(E_{max}/EC_{50})$ values (Supplementary Figures S4D–F). This finding supports the derivation of $\Delta\log(E_{max}/EC_{50})$ from ratiometric HTRF data, minimizing data transformation steps.

To determine whether agonist fingerprinting could be useful in systems with expression of multiple receptors, we examined how $\Delta\log(E_{max}/EC_{50})$ values are affected when more than one β-AR is present. First, we mixed CHO-K1 cells recombinantly expressing either β_1-AR or β_2-AR, at defined ratios of seeding density, and assessed the combined cAMP response. Mixed CHO-K1 β-AR populations produced intermediate agonist fingerprints versus pure expression populations (Figure 2; Supplementary Figure S5; Supplementary Table S2). These data highlight that the $\Delta\log(E_{max}/$

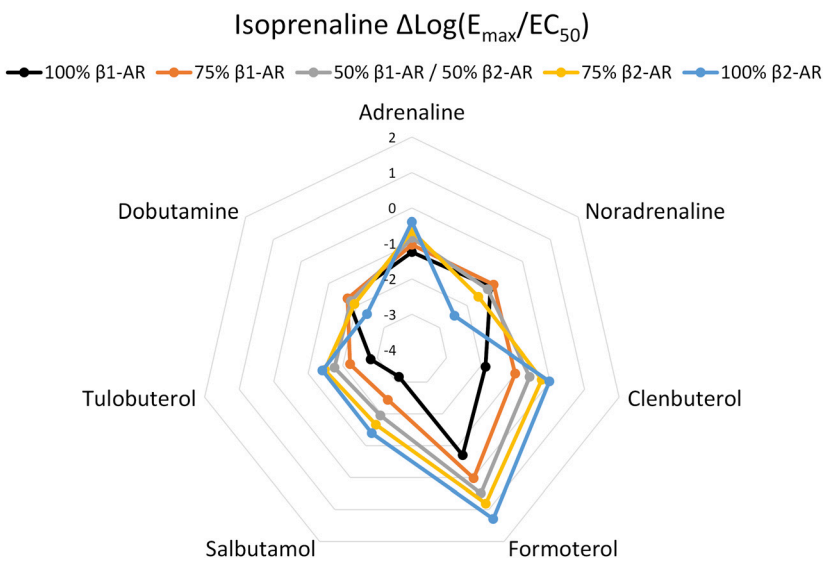

FIGURE 2
Agonist fingerprint derived from functional cAMP curves following admixture of CHO-K1 cells recombinantly expressing either β_1-AR or β_2-AR human receptors. Mixed-expression systems display fingerprints with hybrid features relative to either of the pure expression system.

10.3389/fmolb.2023.1214102

EC_{50}) method of analysis can detect mixed-receptor expression among cell populations.

We then applied this finding to two rat brain cell types which responded to β-AR agonists, but which showed distinctly different agonist fingerprints. First, C6 cells, a rat glioma cell line (Benda et al., 1968), produced a $\Delta\log(E_{max}/EC_{50})$ β-AR agonist fingerprint that did not correspond to either exclusively human β_1-AR or human β_2-AR expression profiles (Figure 3A). To test for expression of multiple β-AR subtypes, we used CRISPR/Cas9 to knockout (KO) either *Adrb1* or *Adrb2* (the rat β_1-AR or β_2-AR genes, respectively) and reassessed functional β-AR expression. C6 *Adrb1* KO cells (Figure 3B) showed a β_2-AR fingerprint, and C6 *Adrb2* KO cells (Figure 3C) showed a β_1-AR-like fingerprint (Figure 3D). Agonist activity differences were detected between rat and human ARs, potentially illustrating the species-dependence of the $\Delta\log(E_{max}/EC_{50})$ metric, as expected for AR homologs of different primary sequences and agonist pharmacology (Strasser et al., 2013; Supplementary Table S2). Mixed β_1-AR and β_2-AR

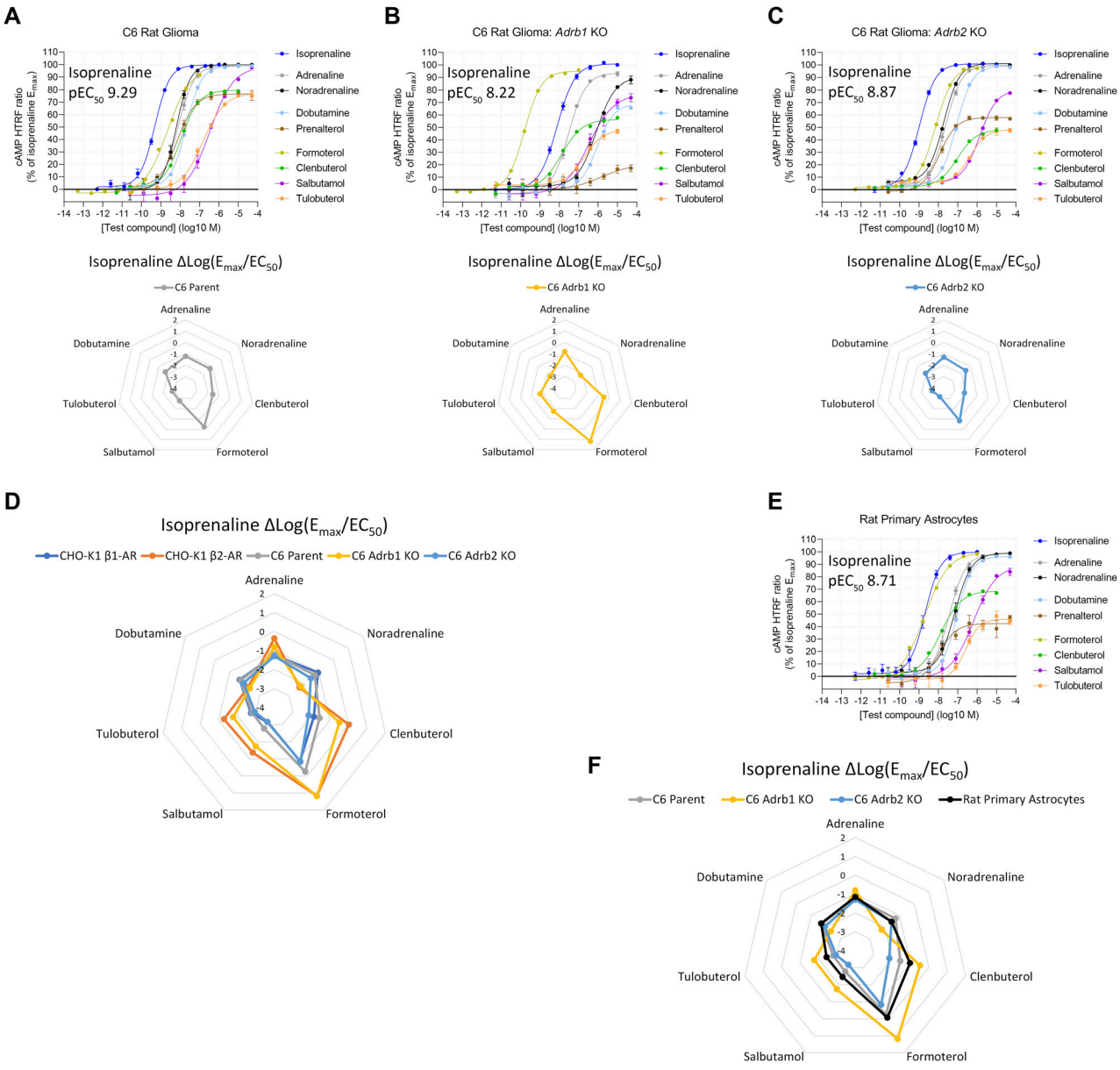

FIGURE 3
Functional cAMP responses to a panel of β-AR agonists in the C6 rat glioma cell line with **(A)** native expression, **(B)** *Adrb1* (β_1-AR) knockout, or **(C)** *Adrb2* (β_2-AR) knockout. Representative curves are displayed, each with four technical replicates, showing mean ± SEM cAMP HTRF responses normalized to the full agonist isoprenaline. Each agonist curve was converted to a $\Delta\log(E_{max}/EC_{50})$ agonist fingerprint using isoprenaline as the reference molecule. Radar plots below the concentration–response curves demonstrate an agonist fingerprint of the C6 cell line non-overlapping with human β_1-AR or β_2-AR receptors, suggesting possible species differences and/or dual-receptor expression. **(D)** Overlay of agonist fingerprints across species for single-receptor systems from either rat (C6 knockout) or human (CHO-K1 recombinant), with an intermediate profile from the C6 co-expressing cell line. **(E)** Rat primary astrocytes display agonist responses and an agonist fingerprint with hybrid features **(F)**, indicating endogenous co-expression of β_1-AR and β_2-AR.

expression was also identified in rat primary cortical astrocytes (Figures 3E, F). These examples demonstrate that endogenous mixed-receptor expression within a single cell type can be identified using an agonist fingerprinting method and supports previous *in vivo* findings suggesting dual expression of rat brain β_1-AR and β_2-AR (Rainbow et al., 1984). Notably, increased β_1-AR subtype expression vs. β_2-AR in rat brain compared to the human brain has been reported (Reznikoff et al., 1986; Joyce et al., 1992).

THP-1 human monocytes are reported to express either β_1-AR (Talmadge et al., 1993) or β_2-AR (Wang et al., 2015; Grisanti et al., 2016; Noh et al., 2017). In contrast to 1321N1 cells, we observed a β-AR agonist response in THP-1 human monocytes, suggestive of β_1-AR expression (Figure 4A). However, a reproducibly shallow Hill slope of formoterol (mean of 0.73, Supplementary Table S2), clenbuterol (0.51), and tulobuterol (0.59), β_2-AR selective agonists, prevented complete agonist fingerprinting (Figure 4A, lower panel) and increased the possibility of multiple β-AR subtypes. To test this possibility, we knocked out expression of either the ADRB1 or ADRB2 genes. In ADRB1 KO THP-1 cells, β-AR agonist activity consistent with β_2-AR expression was detected (Figure 4B). ADRB2 KO THP-1 cells displayed activity consistent with β_1-AR expression, and the average Hill slope of formoterol increased to near unity (1.04) (Figure 4C). Superimposing THP-1 and CHO-K1 $\Delta\log(E_{max}/EC_{50})$ β-AR agonist fingerprints confirmed functional expression of the respective receptors in KO lines (Figure 4D). We noted that, unlike formoterol, the average Hill slopes for clenbuterol (0.53) and tulobuterol (0.78) remained shallow in ADRB2 KO THP-1 cells, perhaps indicating detection of efficacy at two purportedly distinct sites of β_1-AR (Baker, 2005; Baker et al., 2014).

The close alignment between β-AR agonist fingerprints from THP-1 and ADRB2 KO THP-1 cells suggested that β_1-AR contributes the majority of overall cAMP production. Indeed, comparison of the cAMP response to isoprenaline between native (unmodified), ADRB1 KO, and ADRB2 KO THP-1 cells revealed THP-1 ADRB1 KO cells retain only 5% ± 2% of the cAMP response observed in native THP-1 cells (Figure 4E). In contrast, THP-1 ADRB2 KO cells retain most of their cAMP response (87% ± 18%)

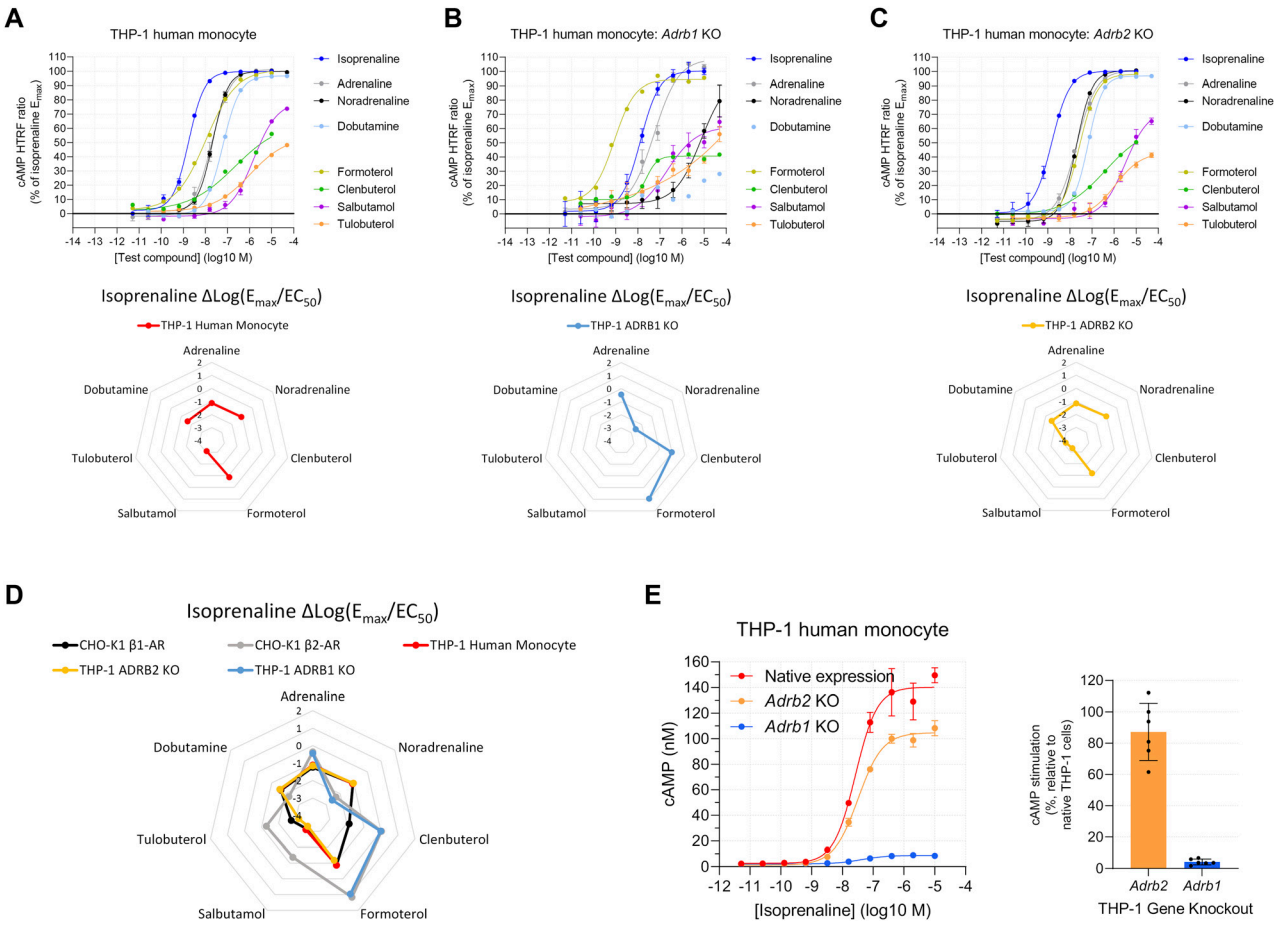

FIGURE 4
Functional cAMP responses to a panel of β-AR agonists in the human THP-1 cell line with **(A)** native expression, **(B)** *Adrb1* (β_1-AR) knockout, or **(C)** *Adrb2* (β_2-AR) knockout. Representative curves are displayed, each with four technical replicates, showing mean ± SEM cAMP HTRF responses normalized to the full agonist isoprenaline. Each agonist curve was converted to a $\Delta\log(E_{max}/EC_{50})$ agonist fingerprint using isoprenaline as the reference molecule. Radar plots below the concentration–response curves reveal an agonist fingerprint of the THP-1 cell line, suggestive of predominantly β_1-AR function. **(D)** Overlay of agonist fingerprints across human cell lines with either endogenous or exogenous receptor expression shows good agreement for single-receptor systems. **(E)** Gene knockout of individual receptors in the THP-1 cell line confirms that the functional cAMP response in parental THP-1 cells is driven predominantly by β_1-AR receptors; the left subpanel shows cAMP concentration after normalization of the HTRF response.

(Figure 4E). These data highlight the predominant expression of β_1-AR over β_2-AR in native THP-1 cells. Although functional β_2-AR expression is low in THP-1 cells, the ADRB1 KO THP-1 system demonstrates that, with sufficient response detected, $\Delta\log(E_{max}/EC_{50})$ values remain consistent in low-expression systems.

3.3 β_2-AR is expressed across a wide range of human brain cell types

After validating the agonist fingerprinting method across a range of expression levels and mixed-receptor systems, we used it to characterize β-AR expression across human cell systems of cerebral origin. We observed functional β_2-AR expression in primary astrocytes isolated from either the cortex or the hippocampus (Figure 5A), primary pericytes from two commercial sources, primary brain vascular smooth muscle cells, and iPSC-derived microglia (Supplementary Figure S6A). Two human immortalized cell lines, cerebral microvascular endothelial cells (HBEC-5i) and microglia (HMC3), also expressed functional β_2-AR (Supplementary Figure S6B), as did a neural progenitor cell line derived from the human cortex (ReNcell CX) (Supplementary Figure S6C). In contrast, neural progenitor cells derived from the ventral mesencephalon (ReNcell VM) did not naturally express high enough levels of functional β-AR to characterize the response but did show a robust β_2-AR response when stably expressing an ADRB2 transgene (Supplementary Figure S6D), highlighting that β-AR second-messenger machinery is functional. When comparing agonist fingerprints, we observed β_2-AR expression to be the predominant functional β-AR subtype in the range of human brain cells studied (Figures 5B, C).

3.4 ΔLog(E_{max}/EC_{50}) measurements in β-arrestin recruitment assay reveal no evidence for β_2-AR ligand bias

A system-independent output allows meaningful interpretation across two signaling pathways, in assays with differing sensitivity. We observed a cAMP response caused by isoprenaline and tulobuterol in CHO-K1 cells expressing modified proteins designed to measure β-arrestin recruitment (Zhao et al., 2008; DiscoverX PathHunter®; Bassoni et al., 2012) (Figure 6A). In the same cell line, β-arrestin recruitment for isoprenaline and tulobuterol was comparatively lessened, displaying a right-shifted isoprenaline potency (pEC_{50} = 7.3 ± 0.2), and lower E_{max} for the partial agonist tulobuterol (Figure 6B). These shifts could indicate decreased assay sensitivity for the β-arrestin readout or could reflect preferential signaling toward one pathway over another. To test this, we transformed agonist response parameters to $\Delta\log(E_{max}/EC_{50})$ and observed a similar agonist fingerprint with tulobuterol as an outlier (Figure 6C). As $\Delta\log(E_{max}/EC_{50})$ removes system-dependent effects, deviation from the line of identity in a plot of $\Delta\log(E_{max}/EC_{50})_{arrestin}$ vs. $\Delta\log(E_{max}/EC_{50})_{cAMP}$ represents ligand bias (Andresen, 2011; Rajagopal et al., 2011; Reiter et al., 2012; Ippolito and Benovic, 2021). In a panel of eight β-AR agonists,

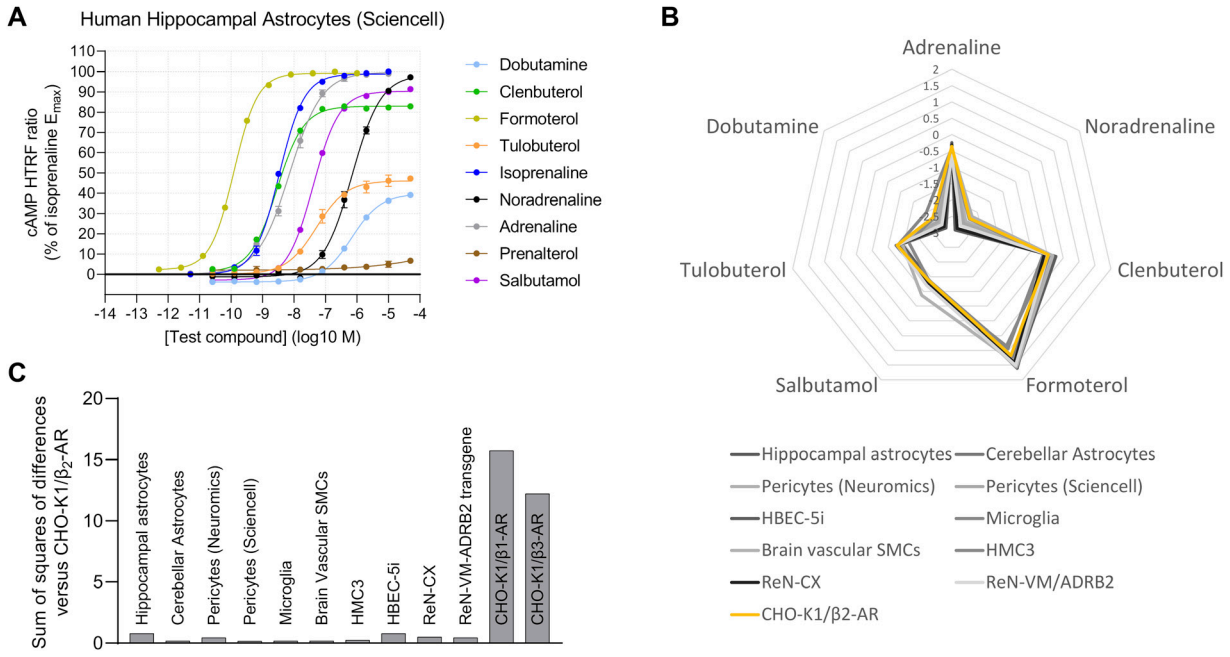

FIGURE 5
Human brain-derived cells display predominantly β_2-AR activity. **(A)** Functional cAMP responses to a panel of β-AR agonists in primary human hippocampal astrocytes, a representative concentration–response curve from examination of several types of brain-derived human primary cells and cell lines. Representative curves are displayed, each with four technical replicates, showing mean ± SEM cAMP HTRF responses normalized to the full agonist isoprenaline. **(B)** The human brain cells tested have agonist fingerprints like those of recombinant CHO-K1/β_2-AR cells, suggestive of predominantly β_2-AR endogenous function. **(C)** Similarity of each agonist fingerprint to the CHO-K1/β_2-AR system by summing the squares of differences for each agonist $\Delta\log(E_{max}/EC_{50})$ value.

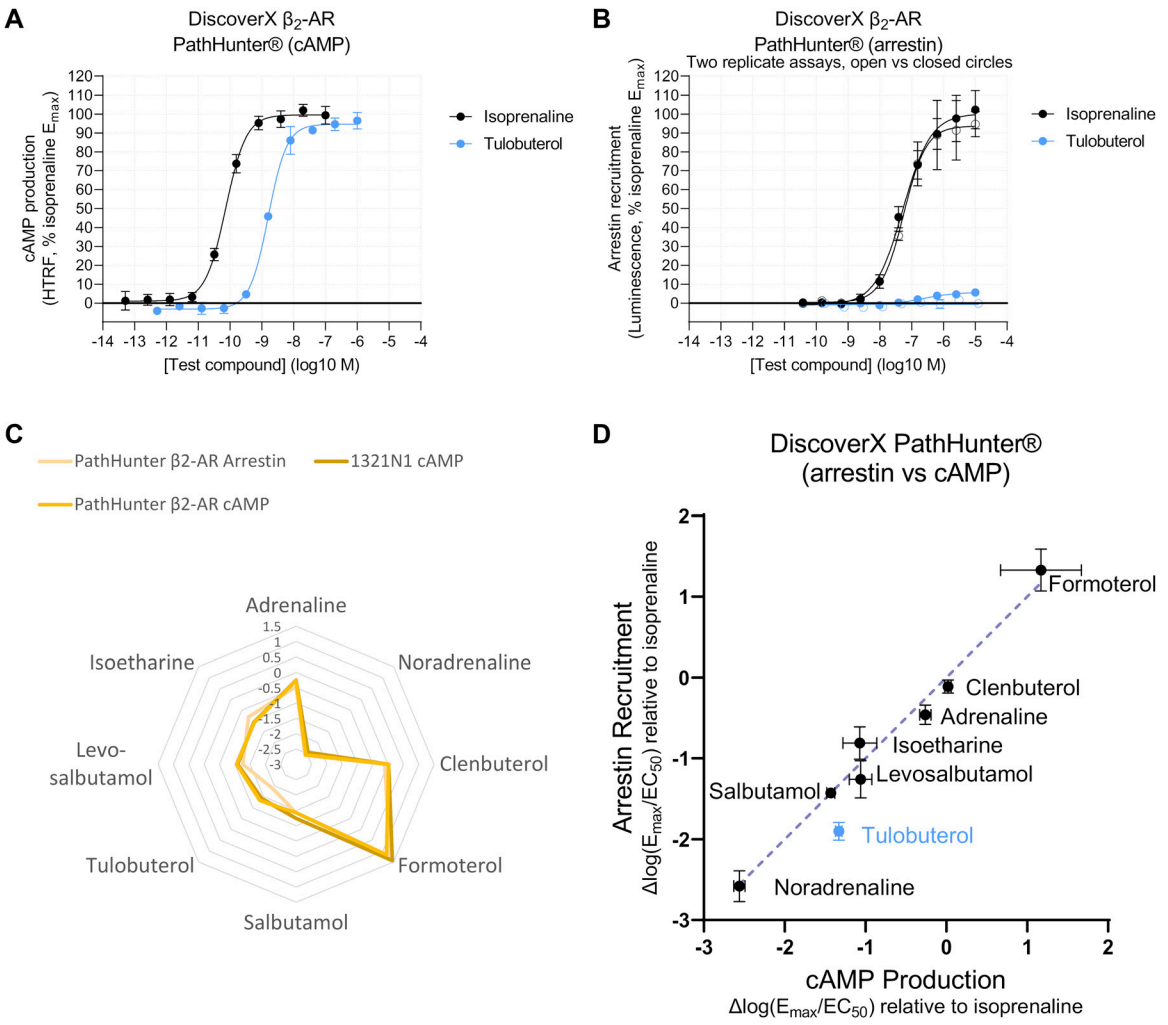

FIGURE 6
Agonist fingerprints comparing distinct signaling pathways suggest that several β_2-AR agonists are unbiased. **(A)** Functional Gs-coupled cAMP production response to full (isoprenaline) and partial (tulobuterol) agonists in PathHunter® β_2-AR cells. Representative curves are displayed, each with four technical replicates, showing mean ± SEM cAMP HTRF responses normalized to the full agonist isoprenaline. **(B)** Arrestin recruitment in PathHunter® β_2-AR cells shows a right-shifted isoprenaline potency and decreased tulobuterol E_{max}, consistent with reduced sensitivity for the arrestin-coupled readout, which leads to poor consistency in the response for weaker agonists such as tulobuterol (two example replicate curves are shown in open versus closed circles to demonstrate day-to-day variability). Summary data of additional replicates are shown in Supplementary Table S2. **(C)** Overlay of agonist fingerprints reveals similarities between arrestin recruitment and cAMP production measured in the same, or in an endogenous, expression system. **(D)** To compare just two signaling pathways, a linear correlation in $\Delta\log(E_{max}/EC_{50})$ values shows potential signaling bias as a deviation from the line of identity. Calculations of $\Delta\Delta\log(E_{max}/EC_{50})$ bias factors are shown in Supplementary Table S4.

seven fell upon the line of identity (Figure 6D), which represents a bias factor ($\Delta\Delta\log(E_{max}/EC_{50})$ (Rajagopal et al., 2011; Winpenny et al., 2016) of 0. These data suggest these β-AR agonists are unbiased at β_2-AR. The exception was tulobuterol, which is discussed as follows.

The cAMP measurements in PathHunter® cells produced concentration–response curves with Hill slopes greater than 1 (Supplementary Table S2), and, due to this, we ensured that these observations were not influenced by receptor and β-arrestin protein modifications in the PathHunter® cell system. We therefore tested the correlation of $\Delta\log(E_{max}/EC_{50})_{arrestin}$ (PathHunter™) with $\Delta\log(E_{max}/EC_{50})_{cAMP}$ values obtained from 1321N1 cells, which naturally express β_2-AR (Figure 1H; Supplementary Figures S3, S4). The same seven agonists fell on the line of identity when correlating β-arrestin response with cAMP derived from 1321N1 cells (Supplementary Figure S7B). This corroborated our finding in the PathHunter® cell line, indicating that PathHunter® and 1321N1 cells display similar β_2-AR-G coupling (Supplementary Figure S7), and suggests that the β-AR agonists tested do not display evidence of ligand bias at β_2-AR in terms of cAMP stimulation vs. β-arrestin recruitment.

As previously mentioned, the one exception in the PathHunter® data was tulobuterol, which did not fall on the line of identity (Figure 6D). However, tulobuterol was the lowest maximal efficacy compound for which a β-arrestin recruitment curve could be detected, though, in some experimental replicates, a response was barely detectable (Figure 6B). This highlights a significant limitation of the low sensitivity of β-arrestin assays for detecting responses to weaker partial agonists.

3.5 Functional desensitization is a more sensitive β-arrestin readout applicable to endogenous systems

To test whether the apparent ligand bias of tulobuterol was an artifact of low E_{max}, we used an alternate method to assess presumed β-arrestin-mediated activity: functional β-AR desensitization. Functional β-AR desensitization detects a reduced cAMP response in cells pre-treated with β-AR agonists. We pre-treated 1321N1 cells in a dose-response manner with a panel of β-AR agonists (Supplementary Table S2) and, 24 h later, challenged the same cells with a single E_{max} concentration of tulobuterol. The level of cAMP produced by an E_{max} dose is suggested to be proportional to the number of active receptors (Su et al., 1979; Doss et al., 1981); thus, the second agonist treatment ostensibly allows a readout of the remaining active receptors. In this assay, pre-incubated ligands may lead to a desensitized system (most likely via β-arrestin recruitment) that is then less responsive to further agonist stimulation. Accordingly, we observed that β-AR agonist pre-treatment reduced cAMP production upon second agonist stimulation, in a dose-dependent manner. We can define functional desensitization $\Delta\log(E_{max}/EC_{50})$ values using test β-AR agonist desensitization curves expressed as a percentage of isoprenaline-induced desensitization (Figure 7A). Thus, $\Delta\log(E_{max}/EC_{50})$ desensitization values were plotted against $\Delta\log(E_{max}/EC_{50})_{cAMP}$ values, all measured in 1321N1 cells. In agreement with β-arrestin recruitment (PathHunter®) results, we observed that most tested β-AR agonists fell on the line of identity, suggesting these β-AR agonists are unbiased (Figure 7B). Because the functional desensitization assay is more sensitive (compare tulobuterol response in Figure 7A; Figure 6B), tulobuterol gives improved detection of maximal response, falling on the line of identity (Figure 7B), and thus also appears unbiased.

Taken together, our system-independent analysis demonstrates that partial β-AR agonists for cAMP production also show partial agonism for β-arrestin recruitment. Partial β-AR agonists also cause a partial degree of functional desensitization. The panel of agonists presented here display varying strengths in potency and intrinsic activity in both assays, and the use of $\Delta\log(E_{max}/EC_{50})$ transformation indicates a lack of ligand bias.

4 Discussion

The ability to characterize GPCR expression in systems with native levels of expression, transducer coupling, and effector signaling enables robust lead optimization for GPCR drug discovery programs. Here, we present a radar plot visualization for "agonist fingerprinting" of β-AR receptor expression using the $\Delta\log(E_{max}/EC_{50})$ parameter, and we provide real-world examples of the utility of $\Delta\log(E_{max}/EC_{50})$ in assessing new cell systems and measuring potential ligand bias. This work builds on that of others (Winpenny et al., 2016; Kenakin, 2017), particularly where similar representations have been used to visualize receptor selectivity in tissues (Kenakin, 2017) or ligand bias (Herenbrink et al., 2016). Because the $\Delta\log(E_{max}/EC_{50})$ value for a given test agonist–reference agonist pair is a system-independent measure of agonism, regardless of factors such as receptor expression level or signal transduction efficiency, this method provides a functional readout advantage over profiling receptor expression with selective antagonists.

The use of multiple agonists for profiling lessens the chance that the expression of a closely related receptor is missed due to the use of non-selective ligands. However, it is worth noting that potentially

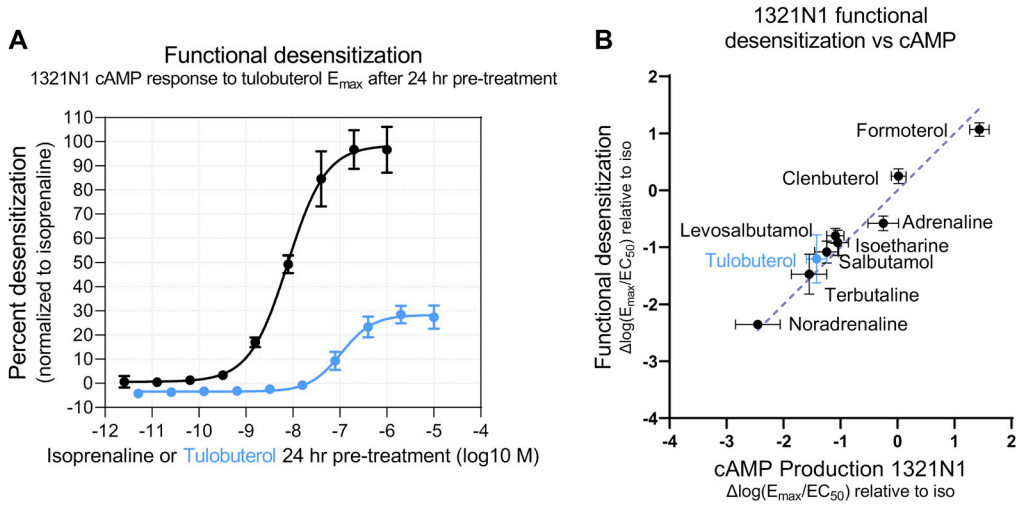

FIGURE 7
Partial agonists desensitize partially in an endogenous expression system. **(A)** Functional desensitization of cAMP production response in 1321N1 cells was calculated by measuring the cAMP produced by a single, fixed concentration of agonist after a 24-h desensitization period of incubation with test agonists across a range of concentrations. Percent desensitization of the partial agonist tulobuterol was normalized to the degree of desensitization induced by the full agonist isoprenaline. Compared with a different arrestin pathway readout in Figure 6, this functional desensitization assay shows a more potent isoprenaline response and a higher maximal tulobuterol response. **(B)** Along the line of identity in a $\Delta\log(E_{max}/EC_{50})$ correlation plot, tulobuterol appears as an unbiased agonist when tested in an arrestin functional assay with higher sensitivity. Calculations of $\Delta\Delta\log(E_{max}/EC_{50})$ bias factors are shown in Supplementary Table S4.

only one test agonist and a single reference agonist may be required for $\Delta\log(E_{max}/EC_{50})$ to be effective in identifying receptor expression, as long as the agonist pair shows a relationship specific to the receptor of interest. For example, the isoprenaline-referenced $\Delta\log(E_{max}/EC_{50})$ value of formoterol is significantly different for β_1-AR (−0.87 ± 0.15), β_2-AR (1.17 ± 0.15), and β_3-AR (−0.02 ± 0.1). To test a novel system, a dose-response of isoprenaline and formoterol and a formoterol $\Delta\log(E_{max}/EC_{50})$ calculation should allow assessment of β-AR subtype expression at a population level, agnostic of the expression level or coupling efficiency of that system. This finding extends the utility of the approach to other receptor types with a limited number of known agonists. Applying agonist fingerprinting to novel systems will be most successful when the assay format allows direct comparison of test and reference agonist (i.e., plate-matching, as in our study) to minimize replicate error in $\Delta\log(E_{max}/EC_{50})$ measurements. To provide an example of measurement error if plate-matching is not possible, we have provided a further analysis of a data subset in Supplementary Table S3.

We observed unique $\Delta\log(E_{max}/EC_{50})$ agonist fingerprints when CHO-K1 cells with single β-AR expression were mixed in different proportions, and the fingerprint changed in a predictable continuum between the pure receptor populations based on those receptor subtype proportions. In addition, we found that rat primary cortical astrocytes, C6 rat glioma cells, and human THP-1 cells naturally express both β_1-AR and β_2-AR, examples of the endogenous expression of multiple β-ARs. The $\Delta\log(E_{max}/EC_{50})$ agonist fingerprint can detect these co-expression scenarios and can even provide clues about the relative expression of receptor subtypes, though this can be difficult to detect when one subtype is expressed more than the other (Figures 2, 3). For example, THP-1 cells naturally express a small population of functional β_2-AR (relative to β_1-AR), which is less obvious in the $\Delta\log(E_{max}/EC_{50})$ β-AR agonist fingerprints. Thus, it is essential to carefully examine the dose–response curves in all situations; a shallow Hill slope from biphasic dose–response curves with selective agonists (such as formoterol for THP-1 cells) was the biggest indicator of potential dual expression.

Expanding $\Delta\log(E_{max}/EC_{50})$ calculations to additional signaling pathways, we show that for β_2-AR, the $\Delta\log(E_{max}/EC_{50})$ value for cAMP production tracks closely with the $\Delta\log(E_{max}/EC_{50})$ value obtained from β-arrestin recruitment and functional desensitization assays across multiple agonists, assayed with PathHunter® and 1321N1 cells, respectively. With the exception of formoterol and levosalbutamol compared in cAMP versus functional desensitization assays, $\Delta\Delta\log(E_{max}/EC_{50})$ values include the value of 0, indicating a lack of bias (Supplementary Table S4). This includes isoetharine, previously reported as β-arrestin-biased (Drake et al., 2008; Ippolito and Benovic, 2021). Our data suggest that at the cellular level, the β_2-AR agonists tested here do not display ligand bias for cAMP signaling or β-arrestin recruitment. This is in line with previous studies, which have noted that different assessments of β_2-AR agonist bias can be derived from different quantification methods and that the magnitude of β_2-AR bias is small (Rajagopal et al., 2011; Onaran et al., 2017) compared to that of other receptors (Winpenny et al., 2016; Onaran et al., 2017).

Our results suggest that meaningful ligand bias is not present among our tested β_2-AR agonists for the functional effects we measured (cAMP, β-arrestin recruitment, and functional desensitization), but this finding may not be generalizable to all tissue types expressing β_2-AR. A major challenge in translating ligand bias to a therapeutic effect is to understand what magnitude of ligand bias in an *in vitro* system corresponds to a clinically meaningful pharmacodynamic effect. Without a clearly biased ligand, this cannot be tested effectively. Therapeutically selective activation of pathways may still be attained by different molecular and therapeutic properties not studied here, namely, lipophilicity, occupancy at equi-effective concentration, and dosing schedule (Düringer et al., 2009). A key takeaway message from our studies and those of others (Düringer et al., 2009) is that, with sustained treatment, unbiased partial agonists desensitize partially. The sensitivity of the target tissue, dosing regimen, and system re-sensitization will determine both the degree of signaling stimulus imparted and its potential for attenuation in therapeutic programs.

In the brain, noradrenaline is released broadly in the cortex and cerebellum in a manner reflecting a 'volume transmission' process, from varicosities on neuronal noradrenergic axons with cell bodies originating mainly in the locus coeruleus (Schwarz and Luo, 2015). Using agonist fingerprinting, we demonstrate β_2-AR expression in human primary pericytes, endothelial cells, vascular smooth muscle cells, cerebral astrocytes, and hippocampal astrocytes. In precursor cell systems, we show β_2-AR expression in iPSC microglia and cortex-derived neural progenitor cells. The observed expression of β_2-AR on several human non-neuronal cell types provides support for this receptor and these cell types as being recipients of noradrenaline volume transmission, in line with observations of multi-cellular expression of β-ARs in the human brain (Shimohama et al., 1987; Kalaria and Harik, 1989; Mantyh et al., 1995; Tsukahara et al., 2018). Our observations that rodent systems show broad dual β_1-AR/β_2-AR expression are also consistent with those of prior tissue analyses (Rainbow et al., 1984; Shao and Sutin, 1992; Asashima et al., 2003). Several groups have mechanistically linked β-ARs with CNS physiology and homeostasis (Gibbs et al., 2009; Catus et al., 2011; Hertz et al., 2013; Coutellier et al., 2014; O'Dell et al., 2015; Hagena et al., 2016; Ardestani et al., 2017), setting the stage for brain active β-AR therapeutics for indications that feature early impairment of locus coeruleus function. Our results show a similar potency for isoprenaline across most cell systems, which may provide a useful translational starting point for achieving a particular pharmacologic response. Successful translation will also require innovative ways to selectively deliver or activate central versus peripheral receptors to achieve target tissue specificity.

Data availability statement

The original contributions presented in the study are included in the article/Supplementary Material; further inquiries can be directed to the corresponding author.

Author contributions

RM, FW, JG, and AF contributed to conception and design of the study. RM, FW, PR, and RR performed the experiments. FW wrote the first draft of the manuscript. RM, FW, and JG wrote the sections of the manuscript. All authors contributed to the article and approved the submitted version.

Funding

Funding for this work was provided by CuraSen Therapeutics, Inc., a clinical-stage biotechnology company focused on activating noradrenaline targets in the central nervous system.

Acknowledgments

The authors would like to thank Dr. Jillian Baker for helpful discussion related to this research.

Conflict of interest

All authors were employed by CuraSen Therapeutics, Inc., at the time of writing. This study received funding from CuraSen Therapeutics, Inc., a clinical-stage biotechnology company focused on activating noradrenaline targets in the central nervous system. The funder had the following involvement with the study: study design; collection, analysis, and interpretation of data; the writing of this article; and the decision to submit it for publication.

Publisher's note

All claims expressed in this article are solely those of the authors and do not necessarily represent those of their affiliated organizations, or those of the publisher, the editors, and the reviewers. Any product that may be evaluated in this article, or claim that may be made by its manufacturer, is not guaranteed or endorsed by the publisher.

Supplementary material

The Supplementary Material for this article can be found online at: https://www.frontiersin.org/articles/10.3389/fmolb.2023.1214102/full#supplementary-material

References

Andresen, B. T. (2011). A pharmacological primer of biased agonism. *Endocr. Metab. Immune Disord. Drug Targets* 11, 92–98. doi:10.2174/187153011795564179

Ardestani, P. M., Evans, A. K., Yi, B., Nguyen, T., Coutellier, L., and Shamloo, M. (2017). Modulation of neuroinflammation and pathology in the 5XFAD mouse model of Alzheimer's disease using a biased and selective beta-1 adrenergic receptor partial agonist. *Neuropharmacology* 116, 371–386. doi:10.1016/j.neuropharm.2017.01.010

Asashima, T., Iizasa, H., Terasaki, T., and Nakashima, E. (2003). Rat brain pericyte cell lines expressing beta2-adrenergic receptor, angiotensin II receptor type 1A, klotho, and CXCR4 mRNAs despite having endothelial cell markers. *J. Cell Physiol.* 197, 69–76. doi:10.1002/jcp.10343

Aston-Jones, G., and Cohen, J. D. (2005). An integrative theory of locus coeruleus-norepinephrine function: Adaptive gain and optimal performance. *Annu. Rev. Neurosci.* 28, 403–450. doi:10.1146/annurev.neuro.28.061604.135709

Baker, J. G., Proudman, R. G. W., and Hill, S. J. (2014). Identification of key residues in transmembrane 4 responsible for the secondary, low-affinity conformation of the human β1-adrenoceptor. *Mol. Pharmacol.* 85, 811–829. doi:10.1124/mol.114.091587

Baker, J. G. (2005). Site of action of beta-ligands at the human beta1-adrenoceptor. *J. Pharmacol. Exp. Ther.* 313, 1163–1171. doi:10.1124/jpet.104.082875

Baker, J. G. (2010). The selectivity of beta-adrenoceptor agonists at human beta1-beta2- and beta3-adrenoceptors. *Brit J. Pharmacol.* 160, 1048–1061. doi:10.1111/j.1476-5381.2010.00754.x

Bari, A., and Robbins, T. W. (2013). Noradrenergic versus dopaminergic modulation of impulsivity, attention and monitoring behaviour in rats performing the stop-signal task: Possible relevance to ADHD. *Psychopharmacology* 230, 89–111. doi:10.1007/s00213-013-3141-6

Bassoni, D. L., Raab, W. J., Achacoso, P. L., Loh, C. Y., and Wehrman, T. S. (2012). Measurements of β-arrestin recruitment to activated seven transmembrane receptors using enzyme complementation. *Methods Mol. Biol.* 897, 181–203. doi:10.1007/978-1-61779-909-9_9

Benda, P., Lightbody, J., Sato, G., Levine, L., and Sweet, W. (1968). Differentiated rat glial cell strain in tissue culture. *Science* 161, 370–371. doi:10.1126/science.161.3839.370

Berridge, C. W., and Waterhouse, B. D. (2003). The locus coeruleus–noradrenergic system: Modulation of behavioral state and state-dependent cognitive processes. *Brain Res. Rev.* 42, 33–84. doi:10.1016/s0165-0173(03)00143-7

Braak, H., Thal, D. R., Ghebremedhin, E., and Tredici, K. D. (2011). Stages of the pathologic process in alzheimer disease: Age categories from 1 to 100 years. *J. Neuropathol. Exp. Neurol.* 70, 960–969. doi:10.1097/nen.0b013e318232a379

Brunnström, H., Friberg, N., Lindberg, E., and Englund, E. (2011). Differential degeneration of the locus coeruleus in dementia subtypes. *Clin. Neuropathol.* 30, 104–110. doi:10.5414/npp30104

Burford, N. T., Watson, J., and Alt, A. (2017). Standard Curves Are Necessary to Determine Pharmacological Properties for Ligands in Functional Assays Using Competition Binding Technologies. *Assay Drug Dev. Techn.* 15, 320–329.

Camoretti-Mercado, B., and Lockey, R. F. (2019). The beta adrenergic theory of bronchial asthma: 50 years later. *J. Allergy Clin. Immun.* 144, 1166–1168. doi:10.1016/j.jaci.2019.07.010

Catus, S. L., Gibbs, M. E., Sato, M., Summers, R. J., and Hutchinson, D. S. (2011). Role of β-adrenoceptors in glucose uptake in astrocytes using β-adrenoceptor knockout mice. *Brit J. Pharmacol.* 162, 1700–1715. doi:10.1111/j.1476-5381.2010.01153.x

Cepeda, M. S., Kern, D. M., Seabrook, G. R., and Lovestone, S. (2019). Comprehensive real-world assessment of marketed medications to guide Parkinson's drug discovery. *Clin. Drug Invest.* 39, 1067–1075. doi:10.1007/s40261-019-00830-4

Coutellier, L., Ardestani, P. M., and Shamloo, M. (2014). β1-adrenergic receptor activation enhances memory in Alzheimer's disease model. *Ann. Clin. Transl. Neur* 1, 348–360. doi:10.1002/acn3.57

Dienel, G. A., and Cruz, N. F. (2016). Aerobic glycolysis during brain activation: Adrenergic regulation and influence of norepinephrine on astrocytic metabolism. *J. Neurochem.* 138, 14–52. doi:10.1111/jnc.13630

Doss, R. C., Perkins, J. P., and Harden, T. K. (1981). Recovery of beta-adrenergic receptors following long term exposure of astrocytoma cells to catecholamine. Role of protein synthesis. *J. Biol. Chem.* 256, 12281–12286. doi:10.1016/s0021-9258(18)43267-x

Drake, M. T., Violin, J. D., Whalen, E. J., Wisler, J. W., Shenoy, S. K., and Lefkowitz, R. J. (2008). beta-arrestin-biased agonism at the beta2-adrenergic receptor. *J. Biol. Chem.* 283, 5669–5676. doi:10.1074/jbc.m708118200

Düringer, C., Grundström, G., Gürcan, E., Dainty, I. A., Lawson, M., Korn, S. H., et al. (2009). Agonist-specific patterns of β2-adrenoceptor responses in human airway cells during prolonged exposure. *Brit J. Pharmacol.* 158, 169–179. doi:10.1111/j.1476-5381.2009.00262.x

Evans, A. K., Ardestani, P. M., Yi, B., Park, H. H., Lam, R. K., and Shamloo, M. (2020). Beta-adrenergic receptor antagonism is proinflammatory and exacerbates neuroinflammation in a mouse model of Alzheimer's Disease. *Neurobiol. Dis.* 146, 105089. doi:10.1016/j.nbd.2020.105089

Feinstein, D. L., Kalinin, S., and Braun, D. (2016). Causes, consequences, and cures for neuroinflammation mediated via the locus coeruleus: Noradrenergic signaling system. *J. Neurochem.* 139, 154–178. doi:10.1111/jnc.13447

Froese, L., Dian, J., Gomez, A., Unger, B., and Zeiler, F. A. (2020). The cerebrovascular response to norepinephrine: A scoping systematic review of the animal and human literature. *Pharmacol. Res. Perspect.* 8, e00655. doi:10.1002/prp2.655

Gibbs, M. E., Rodricks, C. L., Hutchinson, D. S., Summers, R. J., and Miller, S. L. (2009). Importance of adrenergic receptors in prenatally induced cognitive impairment in the domestic chick. *Int. J. Dev. Neurosci.* 27, 27–35. doi:10.1016/j.ijdevneu.2008.10.005

Griffith, D. A., Edmonds, D. J., Fortin, J.-P., Kalgutkar, A. S., Kuzmiski, J. B., Loria, P. M., et al. (2022). A small-molecule oral agonist of the human glucagon-like peptide-1 receptor. *J. Med. Chem.* 65, 8208–8226. doi:10.1021/acs.jmedchem.1c01856

Grisanti, L. A., Traynham, C. J., Repas, A. A., Gao, E., Koch, W. J., and Tilley, D. G. (2016). β2-Adrenergic receptor-dependent chemokine receptor 2 expression regulates leukocyte recruitment to the heart following acute injury. *Proc. Natl. Acad. Sci.* 113, 15126–15131. doi:10.1073/pnas.1611023114

Gronich, N., Abernethy, D. R., Auriel, E., Lavi, I., Rennert, G., and Saliba, W. (2018). β2-adrenoceptor agonists and antagonists and risk of Parkinson's disease. *Mov. Disord.* 33, 1465–1471. doi:10.1002/mds.108

Hagena, H., Hansen, N., and Manahan-Vaughan, D. (2016). β-Adrenergic control of hippocampal function: Subserving the choreography of synaptic information storage and memory. *Cereb. Cortex* 26, 1349–1364. doi:10.1093/cercor/bhv330

Hauser, A. S., Avet, C., Normand, C., Mancini, A., Inoue, A., Bouvier, M., et al. (2022). Common coupling map advances GPCR-G protein selectivity. *Elife* 11, e74107. doi:10.7554/elife.74107

Hayat, H., Regev, N., Matosevich, N., Sales, A., Paredes-Rodriguez, E., Krom, A. J., et al. (2020). Locus coeruleus norepinephrine activity mediates sensory-evoked awakenings from sleep. *Sci. Adv.* 6, eaaz4232. eaaz4232. doi:10.1126/sciadv.aaz4232

Heneka, M. T., Nadrigny, F., Regen, T., Martinez-Hernandez, A., Dumitrescu-Ozimek, L., Terwel, D., et al. (2010). Locus ceruleus controls Alzheimer's disease pathology by modulating microglial functions through norepinephrine. *Proc. Natl. Acad. Sci.* 107, 6058–6063. doi:10.1073/pnas.0909586107

Herenbrink, C. K., Sykes, D. A., Donthamsetti, P., Canals, M., Coudrat, T., Shonberg, J., et al. (2016). The role of kinetic context in apparent biased agonism at GPCRs. *Nat. Commun.* 7, 10842. doi:10.1038/ncomms10842

Hertz, L., Lovatt, D., Goldman, S. A., and Nedergaard, M. (2010). Adrenoceptors in brain: Cellular gene expression and effects on astrocytic metabolism and [Ca2+]i. *Neurochem. Int.* 57, 411–420. doi:10.1016/j.neuint.2010.03.019

Hertz, L., Xu, J., Song, D., Du, T., Yan, E., and Peng, L. (2013). Brain glycogenolysis, adrenoceptors, pyruvate carboxylase, Na+,K+-ATPase and Marie E. Gibbs' pioneering learning studies. *Front. Integr. Neurosci.* 7, 20. doi:10.3389/fnint.2013.00020

Ippolito, M., and Benovic, J. L. (2021). Biased agonism at β-adrenergic receptors. *Cell Signal* 80, 109905. doi:10.1016/j.cellsig.2020.109905

Joyce, J. N., Lexow, N., Kim, S. J., Artymyshyn, R., Senzon, S., Lawerence, D., et al. (1992). Distribution of beta-adrenergic receptor subtypes in human post-mortem brain: Alterations in limbic regions of schizophrenics. *Synapse* 10, 228–246. doi:10.1002/syn.890100306

Kalaria, R. N., and Harik, S. I. (1989). Increased alpha 2- and beta 2-adrenergic receptors in cerebral microvessels in Alzheimer disease. *Neurosci. Lett.* 106, 233–238. doi:10.1016/0304-3940(89)90231-0

Karl, K., Paul, M. D., Pasquale, E. B., and Hristova, K. (2020). Ligand bias in receptor tyrosine kinase signaling. *J. Biol. Chem.* 295, 18494–18507. doi:10.1074/jbc.rev120.015190

Kenakin, T. P. (2017). A system-independent scale (ΔLog(max/EC_{50})) of agonism and allosteric modulation for assessment of selectivity, bias and receptor mutation. *Mol. Pharmacol.* 117, 414–424. doi:10.1124/mol.117.108787

Kenakin, T., Watson, C., Muniz-Medina, V., Christopoulos, A., and Novick, S. (2012). A simple method for quantifying functional selectivity and agonist bias. *Acs Chem. Neurosci.* 3, 193–203. doi:10.1021/cn200111m

Koren, G., Norton, G., Radinsky, K., and Shalev, V. (2019). Chronic use of β-blockers and the risk of Parkinson's disease. *Clin. Drug Invest.* 39, 463–468. doi:10.1007/s40261-019-00771-y

Leanza, G., Gulino, R., and Zorec, R. (2018). Noradrenergic hypothesis linking neurodegeneration-based cognitive decline and astroglia. *Front. Mol. Neurosci.* 11, 254. doi:10.3389/fnmol.2018.00254

Luttrell, L. M., and Lefkowitz, R. J. (2002). The role of beta-arrestins in the termination and transduction of G-protein-coupled receptor signals. *J. Cell Sci.* 115, 455–465. doi:10.1242/jcs.115.3.455

Magistrelli, L., and Comi, C. (2019). Beta2-Adrenoceptor agonists in Parkinson's disease and other synucleinopathies. *J. Neuroimmune Pharm.* 15, 74–81. doi:10.1007/s11481-018-09831-0

Mantyh, P., Rogers, S., Allen, C., Catton, M., Ghilardi, J., Levin, L., et al. (1995). Beta 2-adrenergic receptors are expressed by glia *in vivo* in the normal and injured central nervous system in the rat, rabbit, and human. *J. Neurosci.* 15, 152–164. doi:10.1523/jneurosci.15-01-00152.1995

Matchett, B. J., Grinberg, L. T., Theofilas, P., and Murray, M. E. (2021). The mechanistic link between selective vulnerability of the locus coeruleus and neurodegeneration in Alzheimer's disease. *Acta Neuropathol.* 141, 631–650. doi:10.1007/s00401-020-02248-1

Mather, M., Clewett, D., Sakaki, M., and Harley, C. W. (2016). Norepinephrine ignites local hotspots of neuronal excitation: How arousal amplifies selectivity in perception and memory. *Behav. Brain Sci.* 39, e200. doi:10.1017/s0140525x15000667

Mather, M., and Harley, C. W. (2016). The locus coeruleus: Essential for maintaining cognitive function and the aging brain. *Trends Cogn. Sci.* 20, 214–226. doi:10.1016/j.tics.2016.01.001

Mittal, S., Bjørnevik, K., Im, D. S., Flierl, A., Dong, X., Locascio, J. J., et al. (2017). β2-Adrenoreceptor is a regulator of the α-synuclein gene driving risk of Parkinson's disease. *Science* 357, 891–898. doi:10.1126/science.aaf3934

Noh, H., Yu, M. R., Kim, H. J., Lee, J. H., Park, B.-W., Wu, I.-H., et al. (2017). Beta 2-adrenergic receptor agonists are novel regulators of macrophage activation in diabetic renal and cardiovascular complications. *Kidney Int.* 92, 101–113. doi:10.1016/j.kint.2017.02.013

O'Callaghan, C., Hezemans, F. H., Ye, R., Rua, C., Jones, P. S., Murley, A. G., et al. (2021). Locus coeruleus integrity and the effect of atomoxetine on response inhibition in Parkinson's disease. *Brain* 144, 2513–2526. awab142-. doi:10.1093/brain/awab142

O'Dell, T. J., Connor, S. A., Guglietta, R., and Nguyen, P. V. (2015). β-Adrenergic receptor signaling and modulation of long-term potentiation in the mammalian hippocampus. *Learn Mem.* 22, 461–471. doi:10.1101/lm.031088.113

Onaran, H. O., Ambrosio, C., Uğur, Ö., Koncz, E. M., Grò, M. C., Vezzi, V., et al. (2017). Systematic errors in detecting biased agonism: Analysis of current methods and development of a new model-free approach. *Sci. Rep-uk* 7, 44247. doi:10.1038/srep44247

Rainbow, T. C., Parsons, B., and Wolfe, B. B. (1984). Quantitative autoradiography of beta 1- and beta 2-adrenergic receptors in rat brain. *Proc. Natl. Acad. Sci.* 81, 1585–1589. doi:10.1073/pnas.81.5.1585

Rajagopal, S., Ahn, S., Rominger, D. H., Gowen-MacDonald, W., Lam, C. M., DeWire, S. M., et al. (2011). Quantifying ligand bias at seven-transmembrane receptors. *Mol. Pharmacol.* 80, 367–377. doi:10.1124/mol.111.072801

Reininghaus, N., Paisdzior, S., Höpfner, F., Jyrch, S., Cetindag, C., Scheerer, P., et al. (2022). A setmelanotide-like effect at MC4R is achieved by MC4R dimer separation. *Biomol* 12, 1119. doi:10.3390/biom12081119

Reiter, E., Ahn, S., Shukla, A. K., and Lefkowitz, R. J. (2012). Molecular mechanism of β-arrestin-biased agonism at seven-transmembrane receptors. *Annu. Rev. Pharmacol.* 52, 179–197. doi:10.1146/annurev.pharmtox.010909.105800

Reznikoff, G. A., Manaker, S., Rhodes, C. H., Winokur, A., and Rainbow, T. C. (1986). Localization and quantification of beta-adrenergic receptors in human brain. *Neurology* 36, 1067–1073. doi:10.1212/wnl.36.8.1067

Roozendaal, B., and Hermans, E. J. (2017). Norepinephrine effects on the encoding and consolidation of emotional memory: Improving synergy between animal and human studies. *Curr. Opin. Behav. Sci.* 14, 115–122. doi:10.1016/j.cobeha.2017.02.001

Schwarz, L. A., and Luo, L. (2015). Organization of the locus coeruleus-norepinephrine system. *Curr. Biol.* 25, R1051–R1056. doi:10.1016/j.cub.2015.09.039

Servant, N. B., Williams, M. E., Brust, P. F., Tang, H., Wong, M. S., Chen, Q., et al. (2022). A dynamic mass redistribution assay for the human sweet taste receptor uncovers G-protein dependent biased ligands. *Front. Pharmacol.* 13, 832529. doi:10.3389/fphar.2022.832529

Shao, Y., and Sutin, J. (1992). Expression of adrenergic receptors in individual astrocytes and motor neurons isolated from the adult rat brain. *Glia* 6, 108–117. doi:10.1002/glia.440060205

Shimohama, S., Taniguchi, T., Fujiwara, M., and Kameyama, M. (1987). Changes in β-adrenergic receptor subtypes in alzheimer-type dementia. *J. Neurochem.* 48, 1215–1221. doi:10.1111/j.1471-4159.1987.tb05649.x

Strasser, A., Wittmann, H.-J., Buschauer, A., Schneider, E. H., and Seifert, R. (2013). Species-dependent activities of G-protein-coupled receptor ligands: Lessons from histamine receptor orthologs. *Trends Pharmacol. Sci.* 34, 13–32. doi:10.1016/j.tips.2012.10.004

Su, Y. F., Harden, T. K., and Perkins, J. P. (1979). Isoproterenol-induced desensitization of adenylate cyclase in human astrocytoma cells. Relation of loss of hormonal responsiveness and decrement in beta-adrenergic receptors. *J. Biol. Chem.* 254, 38–41. doi:10.1016/s0021-9258(17)30267-3

Talmadge, J., Scott, R., Castelli, P., Newman-Tarr, T., and Lee, J. (1993). Molecular pharmacology of the beta-adrenergic receptor on THP-1 cells. *Int. J. Immunopharmaco* 15, 219–228. doi:10.1016/0192-0561(93)90098-j

Tewson, P. H., Martinka, S., Shaner, N. C., Hughes, T. E., and Quinn, A. M. (2016). New DAG and cAMP sensors optimized for live-cell assays in automated laboratories. *J. Biomol. Screen* 21, 298–305. doi:10.1177/1087057115618608

Toussay, X., Basu, K., Lacoste, B., and Hamel, E. (2013). Locus coeruleus stimulation recruits a broad cortical neuronal network and increases cortical perfusion. *J. Neurosci.* 33, 3390–3401. doi:10.1523/jneurosci.3346-12.2013

Tsukahara, T., Taniguchi, T., Shimohama, S., Fujiwara, M., and Handa, H. (2018). Characterization of beta adrenergic receptors in human cerebral arteries and alteration of the receptors after subarachnoid hemorrhage. *Stroke* 17, 202–207. doi:10.1161/01.str.17.2.202

Wachter, S. B., and Gilbert, E. M. (2012). Beta-adrenergic receptors, from their discovery and characterization through their manipulation to beneficial clinical application. *Cardiology* 122, 104–112. doi:10.1159/000339271

Wang, W., Zhang, Y., Xu, M., Zhang, Y.-Y., and He, B. (2015). Fenoterol inhibits LPS-induced AMPK activation and inflammatory cytokine production through β-arrestin-2 in THP-1 cell line. *Biochem. Bioph Res. Co.* 462, 119–123. doi:10.1016/j.bbrc.2015.04.097

Winpenny, D., Clark, M., and Cawkill, D. (2016). Biased ligand quantification in drug discovery: From theory to high throughput screening to identify new biased μ opioid receptor agonists. *Brit J. Pharmacol.* 173, 1393–1403. doi:10.1111/bph.13441

Zhao, X., Jones, A., Olson, K. R., Peng, K., Wehrman, T., Park, A., et al. (2008). A homogeneous enzyme fragment complementation-based β-arrestin translocation assay for high-throughput screening of G-protein-coupled receptors. *J. Biomol. Screen* 13, 737–747. doi:10.1177/1087057108321531